Synergistic Effect of $LiPF_6$ and $LiBF_4$ as Electrolyte Salts in Lithium-Ion Cells

L. D. Ellis,[a] I. G. Hill,[b] Kevin L. Gering,[c] and J. R. Dahn[a,b,*,z]

[a]*Department of Chemistry, Dalhousie University, Halifax B3H 4R2, Canada*
[b]*Department of Physics and Atmospheric Science, Dalhousie University, Halifax B3H 4R2,Canada*
[c]*Idaho National Laboratory, Idaho Falls, Idaho 83415-3732, USA*

Recent work shows promise for $LiBF_4$ as an electrolyte salt for high voltage lithium-ion batteries. $LiBF_4$ is more hydrolytically stable than $LiPF_6$, and in some cases has proved to be more stable at high voltage. This work shows that 1.0 M electrolytes consisting of equal parts $LiBF_4$ and $LiPF_6$ have better performance in certain high voltage (4.35 V) lithium-ion cells than electrolytes with $LiPF_6$ or $LiBF_4$ alone. This is shown using long-term cycling and ultra-high precision coulometry on lithium-ion cells, with and without electrolyte additives. Ultra-high precision coulometry showed that electrolyte with 1:1 $LiPF_6$:$LiBF_4$ and no other additives performed as well as electrolyte with $LiPF_6$ and state-of-the-art additive blends in these cells. The synergism between $LiPF_6$ and $LiBF_4$ was explored using XPS, symmetric cells and EIS analysis. These show that $LiBF_4$ reduces impedance growth at the positive electrode, while $LiPF_6$ improves passivation at the negative electrode.

Manuscript received July 28, 2017. Published August 17, 2017.

Recent work has shown that $LiBF_4$ may be a promising alternative salt, or co-salt, for high voltage lithium ion cells.[1–9] $LiBF_4$ has a similar chemical structure to $LiPF_6$, which is the best-known and most widely used electrolyte salt for lithium-ion batteries. Both these salts have different advantages and disadvantages in lithium-ion cells. $LiPF_6$ has high solution conductivity in carbonate solvents, and helps passivate the negative electrode SEI. However, $LiPF_6$ is known to have poor thermal and hydrolytic stability.[10,11] Decomposition of $LiPF_6$ results in the formation of reactive species, notably HF and PF_5, which are thought to cause a cascade of undesirable side-reactions inside the cell.[10–12] $LiBF_4$ has often been studied as a substitute for $LiPF_6$ in lithium-ion cells because of its improved thermal and hydrolytic stability.[3,12–17] $LiBF_4$ has demonstrated several other important advantages over $LiPF_6$: improved performance at sub-zero temperatures, improved passivation of the Al current collector, and improved performance at the positive electrode.[1,3–9,12–14,17] The disadvantages of $LiBF_4$ are lower conductivity compared to $LiPF_6$ and poor performance at the negative electrode.[13,16]

Our previous work explored the use of $LiBF_4$ in machine-made, high voltage, lithium-ion pouch cells.[5] That work showed that at 4.5 V, electrolyte with $LiBF_4$ reacts to cause gas evolution, impedance growth and failure of lithium-ion cells.[5] However, when cycled below 4.4 V, cells with $LiBF_4$ electrolyte produced less gas, and had higher coulombic efficiency (CE) than cells containing $LiPF_6$ alone. Curiously, cells containing equal amounts of $LiPF_6$ and $LiBF_4$ had higher CE than cells containing either $LiPF_6$ or $LiBF_4$ alone. This phenomenon suggests that blends of $LiPF_6$ and $LiBF_4$ salts may improve performance of cells, when cycled below 4.4 V.

The purpose of this study is to further explore the performance of cells containing $LiBF_4$, cycling at voltages below 4.4 V, where $LiBF_4$ was shown to be stable. The effect of electrolyte additives in cells cycling up to 4.4 V with $LiBF_4$ electrolyte was explored (previous work showed that electrolyte additives were ineffective at protecting cells with $LiBF_4$ from gassing and impedance growth at voltages > 4.4 V).[5] The effect of mixing $LiPF_6$ and $LiBF_4$ was studied, to search for the optimum ratio of the two salts. Evaluation of cell performance was done using UHPC and long-term cycling experiments. XPS analysis was done on cycled electrodes to observe how $LiBF_4$ changed the chemical composition of the electrode surfaces. Symmetric cells were constructed out of aged electrodes and cycled to observe how $LiBF_4$ changed the R_{ct} of the positive electrodes. The results of these tests show that $LiBF_4$ reduced the rate of parasitic reactions in the electrolyte, and that $LiBF_4$ is especially beneficial at the positive electrode when cycled below 4.4 V. The performance of full cells was best, based on the compositions studied, when $LiPF_6$ and $LiBF_4$ were used in equal mole ratios. In an attempt to understand the cause of improved cell performance with equimolar salt ratios, electrolyte properties were calculated using Gering's Advanced Electrolyte Model (AEM).[18,19]

Experimental

Electrolyte preparation.—Electrolyte preparation was done in an Ar-filled glove box to ensure minimal exposure to moisture and oxygen. 1 M electrolyte solutions were prepared by dissolving $LiPF_6$ and/or $LiBF_4$ salts (BASF, 99.94%, water content <14 ppm) in a 3:7 weight ratio of EC:EMC solvent (BASF, water content < 20 ppm). The salt was weighed on an analytical balance and transferred to a vial. The amount of solvent needed to make a 1 M solution was added to the vial using a micro pipette, with an accuracy of ±0.01 mL. The following additives were added to the electrolyte in amounts of 2 wt%: vinylene carbonate (VC, BASF, 99.97%) and prop-1-ene-1,3-sultone (PES, Lianchuang Medicinal Chemistry Co., Ltd., China, 98.20%). A ternary blend of additives containing 2 wt% PES, 2 wt% 1,3,2-dioxathiolan-2,2-oxide (DTD, YaCoo, > 98%) and 2 wt% tris(trimethlysilyl) phosphite (TTSPi, TCI, 95%), abbreviated henceforth as "PES222", was also used. Electrolyte without additives is henceforth referred to as "control".

Cell construction.—Machine made lithium-ion pouch cells were obtained without electrolyte from Li-Fun Technology (Xinma Industry Zone, Golden Dragon Road, Tianyuan District, Zhuzhou City, Hunan Province, PRC, 412000). The negative electrode of these cells was 96% artificial graphite particles (15–30 μm), 2% carbon black conductive diluent and 2% sodium carboxymethylcellulose (NaCMC)/styrene butadiene rubber (SBR) binder. The positive electrode was 96% $Li[Ni_{0.4}Mn_{0.4}Co_{0.2}]O_2$ (NMC442) particles (5–15 μm, Umicore, Korea), 2% carbon black conductive diluent and 2% polyvinylidene fluoride (PVDF) binder. The ratio of negative/positive electrode capacity allowed for cell voltages of 4.7 V to be reached without lithium plating, delivering a capacity of 250 mAh. Prior to filling with electrolyte, the cells were opened and dried under vacuum at 80°C for 14 hours, to remove residual moisture. The cells were then transferred to an Ar-filled glove box, without exposure to air. To each cell a slight excess, 0.8 mL, of electrolyte was added. The aluminium-laminate cell casings were sealed by heat crimping at 150°C under a gauge pressure of −90 kPa using a (Model MSK-115 V from MTI Corp.) vacuum sealer.

*Electrochemical Society Fellow.
[z]E-mail: jeff.dahn@dal.ca

Archimedes volume change measurements.—The volume of gas generated by cycling was quantified by subtracting the weight of the cells submerged under liquid before and after gas-forming reactions, according to Archimedes' principle. Details of the Archimedes volume measurement instrument at Dalhousie University can be found in several publications.[20–22] Archimedes volume measurements were taken before and after the first and second degas steps (described in the Cell formation sections below) for cells undergoing UHPC cycling and storage to determine the amount of gas formed by reactions of the electrolyte with the anode and cathode, respectively. In-situ Archimedes volume measurements were performed on cells that were cycled at 40.0 ± 0.1° C, using a Neware (Shenzhen, China) charging system. Cells destined for in-situ volume measurements underwent wetting, cell formation to 3.5 V and the first degas, according to the standard protocol described below. After degassing, the cells were loaded into the in-situ Archimedes measurement system and to complete their formation cycle, as described below.

Cell formation: wetting.—After filling with electrolyte, the cells were held at 1.5 V for 24 hours. This allowed time for the electrolyte to permeate through the separator and electrodes. The voltage of 1.5 V was applied to prevent oxidation of the copper current collector, which occurs above 3.2 V vs Li/Li^+. [23] All cells were clamped between rubber blocks during the formation, cycling and EIS tests which followed to ensure stack pressure on the electrodes. The pressure applied was > 0.4 atm.

Cell formation; first degas.—The cells were then transferred to a 40.0 ± 0.1°C temperature controlled box, where they were cycled with a Maccor 4000 series charger. All duplicate cells in this study underwent the formation cycling connected in parallel, unless indicated otherwise. The currents specified are the currents per cell (half the current applied per cell pair). The cycling procedure began with an 11 mA (C/10) charge to 3.5 V, followed by a 1 hour constant voltage hold at 3.5 V. During this step, EC and other electrolyte components are reduced, forming the initial SEI on the negative electrode and creating gaseous by-products. If the volume of gas produced exceeded 0.2 mL, cells were transferred to an Ar-filled glove box, where they were "degassed" by opening and resealing the laminate cell casings under vacuum.

Cell formation; second degas.—The cells were returned to their temperature controlled box, where they were charged at 11 mA to 4.35 V. The voltage was held at this value for 1 hour, to equilibrate the cells at this potential. The cells were then discharged at 11 mA to 3.8 V and held at this potential for 1 hour. The cells were removed from the temperature controlled box for Archimedes volume measurements and degassed a second time if the volume of gas produced exceeded 0.2 mL.

Electrochemical impedance spectrometry (EIS).—EIS measurements were taken before and after cycling and storage tests. EIS measurements were performed at 10.0 ± 0.1°C, using a BioLogic VMP3 potentiostat to induce a 10 mV sinusoidal bias at frequencies ranging from 10 mHz to 100 kHz. The magnitude of the charge transfer impedance, R_{ct}, was obtained by determining the diameter of the mid-frequency semicircle in the Nyquist plot.[24–26] This region accounts for the interfacial contributions to impedance, such as the intrinsic SEI resistivity, porous effects, lithium desolvation process, and others.

Ultra-high precision coulometry (UHPC) cycling.—After formation, cells destined for cycling were loaded into 40.0 ± 0.1°C temperature controlled boxes and cycled with a UHPC system (made in-house).[27] The UHPC system was designed and built at Dalhousie University, as described in several publications.[27,28] All cells were cycled, with clamps using a continuous cycling protocol. The continuous cycling test consisted of constant current cycling, at a rate of 10 mA, between 2.8 V and 4.4 V. The same currents in the same potential ranges were used during discharge.

Long-term cycling.—After UHPC cycling, cells with control electrolyte and cells with PES222 additive were cycled on a Neware battery cycler (Shenzhen, China). Cells were tested either at 40°C or 55°C. Cells were cycled using a constant current of C/3, between 2.8 and 4.35 V. Every 25th cycle was done at a slower rate of C/20.

Symmetric cells.—After UHPC cycling, cells with control electrolyte, equilibrated at 3.8 V, were dissected in an Ar-filled glove box. Disks with a 1 cm^2 diameter were punched from single side coated regions of the negative and positive electrodes and rinsed with EMC solvent to remove residual $LiPF_6$ and EC. Symmetric cells were made by assembling two electrodes of the same type in 2325-type coin cells, using microporous polypropylene (Celgard 2301) and blown-microfiber (3 M Co) as separators and the same electrolyte as the parent cell. Cycling of symmetric cells was done on a Maccor series 4000 battery cycler, at a rate of C/10, between −0.5 V and +0.5 V (corresponding to full cell voltages of 3.25 V and 4.25 V), at 40°C.

X-ray photoelectron spectroscopy (XPS).—Lithium-ion pouch cells were transferred to an Ar-filled glove box. The electrodes were removed, and rinsed several times with EMC, to remove $LiPF_6$ and EC that precipitate from liquid electrolyte solutions. Removal of these species is essential for the underlying SEI components to be observed by XPS. Removal of EC and $LiPF_6$ is also important for maintaining low pressures in the XPS system, and preventing damage to the detector from $PF_{5\,(g)}$ (generated from the thermal decomposition of $LiPF_6$ under unmonochromatized radiation). Rinsing with EMC is not expected to dissolve any SEI components, as EMC is the major component of the electrolyte in which the SEI was formed. Once the rinsed samples were dried, they were mounted onto a molybdenum sample holder, using double-sided, ultra-high vacuum-compatible copper tape. The sample holder was then transferred into the XPS system, without exposure to air, using a specially designed air-tight apparatus that could be evacuated to low pressures. Electrodes were left under ultra-high vacuum overnight to allow for off-gassing of any remaining volatile components. The samples were then transferred to the analysis chamber of the XPS, which has a base pressure of 1×10^{-10} mbar and was maintained below 2×10^{-9} mbar during the experiments. Analysis was performed with a SPECS spectrometer equipped with a Phoibos 150 hemispherical analyzer, using unmonochromatized Mg Kα radiation and a pass energy of 20 eV. Preliminary and final survey scans were compared to ensure that no photochemical degradation was induced during analysis. Data analysis was done using CasaXPS software (v. 2.3.18). Charge correction was done by fitting the adventitious carbon peak, and shifting the x-axis such that this peak fell at 285.0 eV. XPS spectra were fit with a non-linear Shirley-type background. This background was subtracted from the signal to allow for qualitative comparison of atomic concentrations between samples using relative peak heights. Peaks were fit with a mixed Gaussian (70%) /Lorentzian (30%) line shape. Uncertainties for the quantification of elements were calculated by the CasaXPS software, using the intensity of the quantification regions and the surrounding noise.

Results and Discussion

Figure 1 shows in-situ gas evolution data. Voltage and gas volume vs. time, are shown for cells with increasing amounts of $LiBF_4$, undergoing the second stage of their formation cycle, at 40 C. Figure 1 shows that increasing amounts of $LiBF_4$ result in less gas evolution above 3.5 V. The addition of even a small amount of $LiBF_4$ eliminates the gas-evolving reaction occurring at 3.6 V in cells with $LiPF_6$ electrolyte.

Figure 2 shows UHPC cycling data. Cells were cycled to 4.35 V at 40°C and approximately C/20. Cells containing $LiPF_6$, $LiBF_4$ or mixtures of both $LiPF_6$ and $LiBF_4$ were tested. The effects of electrolyte additives, 2% VC and PES222, are shown. Figure 2a

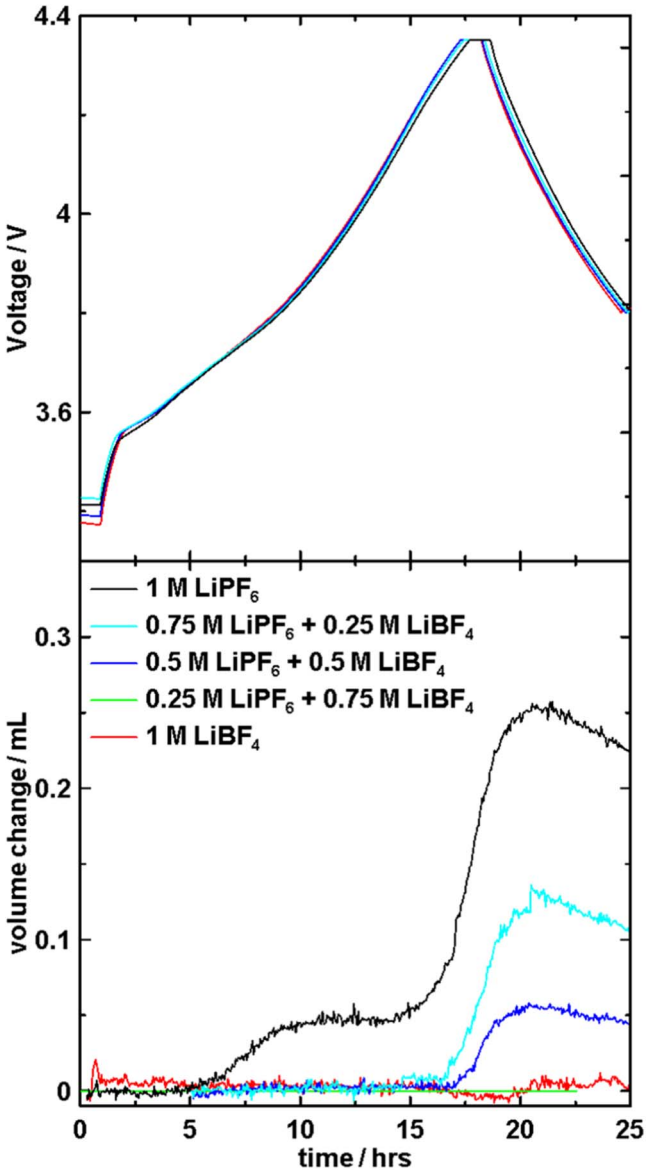

Figure 1. Voltage vs. time and volume change vs. time for cells with 1 M control electrolyte and various ratios of $LiPF_6$:$LiBF_4$, undergoing the second step of the formation cycle to 4.35 V, at a rate of C/20, at 40°C.

shows CE vs cycle number. In all cases, cells with $LiPF_6$ had the lowest CE after 20 cycles, followed by cells with $LiBF_4$. In all cases, cells with both $LiPF_6$ and $LiBF_4$ have the highest CE after 20 cycles. In cells with control electrolyte, without electrolyte additives, the benefit of $LiBF_4$ is the most pronounced. After 20 cycles, cells with a mixture of $LiPF_6$ and $LiBF_4$ in control electrolyte without electrolyte additives have a CE of ~0.9975. This is only slightly less than the coulombic efficiency of cells with $LiPF_6$ and PES222 electrolyte (0.998), which is considered to be a relatively effective electrolyte blend for high voltage NMC442/graphite cells.[29] In addition, Figure 2a shows that cells with 0.5 M $LiPF_6$ and 0.5 M $LiBF_4$ and PES222 have higher CE than cells with $LiPF_6$ alone. This suggests that the inclusion of a certain amount of $LiBF_4$ to electrolytes is very effective when cells are cycled below 4.4 V.

Figure 2b shows the cumulative charge end-point capacity slippage (slipC) of cells containing $LiPF_6$, $LiBF_4$ or a mixture of $LiPF_6$ and $LiBF_4$ cycled to 4.35 V. In control cells, without electrolyte additives, and in cells with 2% VC, a mixture of $LiPF_6$ and $LiBF_4$ results in the lowest amounts of charge end-point capacity slippage, ~8 mAh after 20 cycles. This result is consistent with other studies, which have shown that organic carbonate solutions of $LiBF_4$ are more stable at high voltage than those of $LiPF_6$.[1,3,4,8,9] Figure 2c shows discharge capacity vs cycle number for the same cells. Figure 2c demonstrates that increasing the amount of $LiBF_4$ decreases the reversible capacity. It was shown in previous work that $LiBF_4$ increases the irreversible capacity of the first cycle.[5] The use of electrolyte additives, 2% VC and PES222, somewhat reduces the first cycle irreversible capacity loss of cells containing $LiBF_4$. Figure 2d shows the voltage hysteresis, ΔV, vs cycle number. Cells with $LiBF_4$ alone have higher ΔV, while cells with $LiPF_6$, or a mixture of $LiBF_4$ and $LiPF_6$ have similarly small ΔV.

Figure 3 shows the charge-transfer resistance, R_{ct}, of cells with control electrolyte, before and after UHPC cycling. R_{ct} was taken to be the diameter of the mid-frequency semicircle of the Nyquist plot. Figure 3 shows that R_{ct} of cells with $LiPF_6$ is low, and remains low after 20 UHPC cycles. In cells with $LiBF_4$, R_{ct} is high, nearly double that of the cells with $LiPF_6$, and R_{ct} nearly doubles after 20 UHPC cycles. It was shown in the previous work $LiBF_4$ causes increased R_{ct} at the negative electrode.[5]

After 20 UHPC cycles, control cells and cells with PES222 were subjected to long-term cycling. Due to limited testing channel space, control cells and cells with PES222 were tested at different temperatures: control cells were cycled at 40°C and cells with PES222 were cycled at 55°C. Figure 4a shows discharge capacity vs cycle number for control cells, without additives, cycled at 40°C. The cell with 1 M $LiPF_6$ was the first to fail, reaching 80% capacity retention after 400 cycles. The cell with 0.75 M $LiPF_6$ and 0.25 M $LiBF_4$ was the next to fail, reaching 80% capacity loss after 650 cycles. The cells with 1 M $LiBF_4$, 1:1 and 1:3 ratios of $LiPF_6$:$LiBF_4$ continued to cycle beyond 600 cycles, with 90% capacity retention. After 650 cycles, all cells were removed from the charger, due to limited charger channel availability. These long-term cycling results generally agree with UHPC cycling predictions, which showed that cells with $LiPF_6$ have lower CE than cells with $LiBF_4$ or mixtures of $LiBF_4$ and $LiPF_6$, when cycled to 4.35 V. It is not understood why cells with a 3:1 ratio of $LiPF_6$:$LiBF_4$ lose more capacity during long-term cycling than cells with 1:1 or 1:3 ratios of $LiPF_6$: $LiBF_4$, when those cells all had similar CE during UHPC cycling. Figure 4b shows discharge capacity vs cycle number for cells with PES222 cycled at 55°C. Cells with 1 M $LiPF_6$, 0.5 M $LiPF_6$ and 0.5 M $LiBF_4$, and 1 M $LiBF_4$ all reach ~80% capacity retention after 300 cycles. This agrees with UHPC results, which showed very similar CE and charge-end point slippage for all cells with PES222.

After 20 UHPC cycles, several control cells, without additives were dissected for XPS analysis and the construction of symmetric cells. Figure 5 shows photographs of the separators and of the tape from the outside of the jelly roll. Figure 5 shows significant discoloration of the separator and tape from cells with $LiPF_6$. The separator from the cell with $LiPF_6$ was browned, especially in areas which contacted the active electrode materials. In addition to browning, the separator from the cell with $LiPF_6$ was coated with a "slime", even in areas which did not contact the active electrode material. The tape from the cell which contained $LiPF_6$ was no longer adhesive. The tape bleached from green to a yellow color, especially where the edge of the positive electrode had been. This indicates that the chemical which caused the bleaching originated from inside the jelly roll. A corresponding yellow stain was observed on the separator, in the location which had been opposite the tape in the jelly roll. The cell with a 1:1 blend of $LiPF_6$ and $LiBF_4$ showed the same discolorations, but to a lesser degree. The cell with $LiBF_4$ alone showed very faint discoloration of the separator and was not slimy. The tape from the cell with $LiBF_4$ retained its original green color and adhesive properties. Though the cause of this discoloration is unknown, there is reason to believe that it is caused by the presence of $LiPF_6$. The reaction of $LiPF_6$ with trace water can create HF, which is very corrosive.[10] HF can initiate further electrolyte decomposition reactions, which could cause the discolorations shown in Figure 5.

Figure 6 shows the cycling of positive-positive symmetric cells, which were made from the electrodes harvested from control cells,

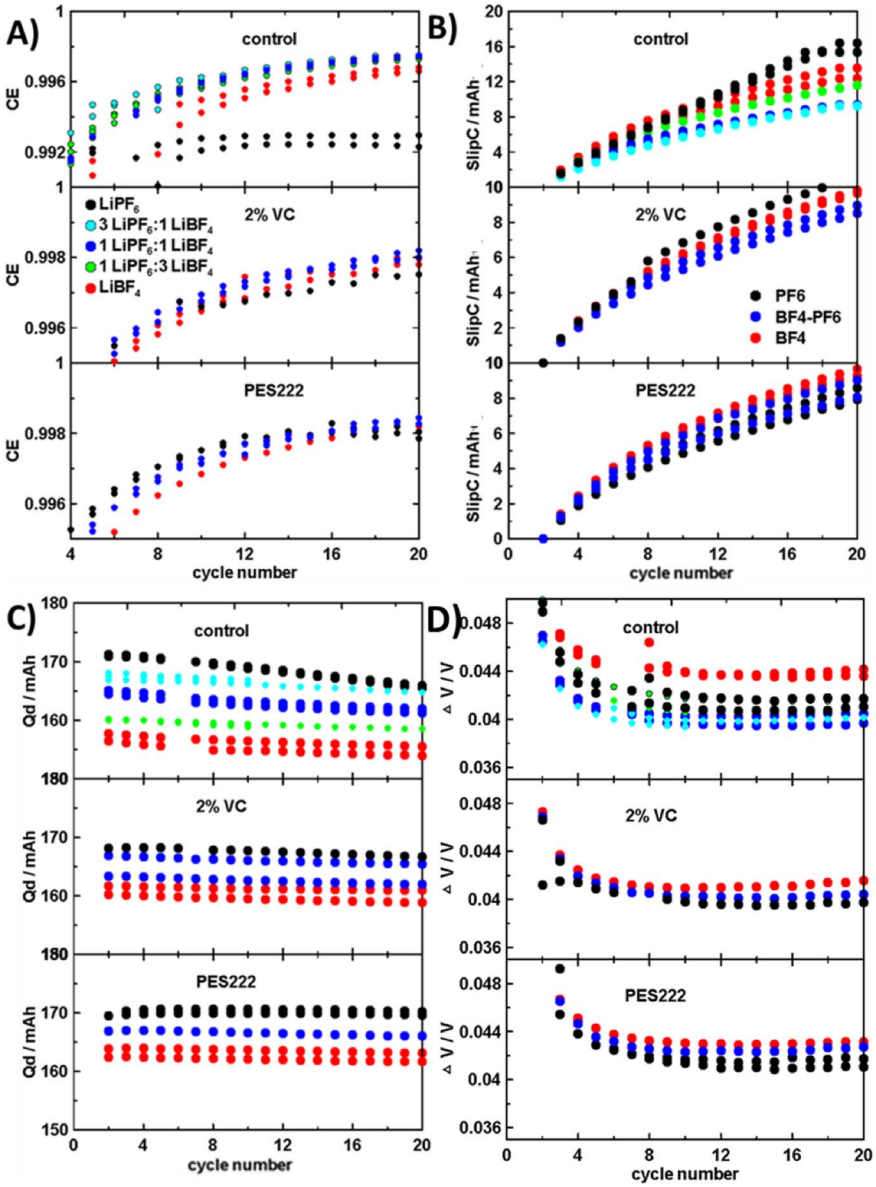

Figure 2. a) CE, b) cumulative charge-end point slippage (slipC), c) discharge capacity (Qd), and d) delta V for cells undergoing UHPC cycling to 4.35 V, at a rate of C/20, at 40°C without additives (control), with 2% VC, and PES222.

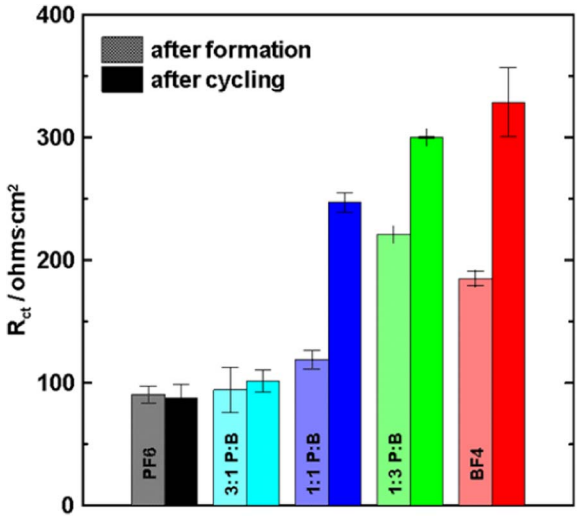

Figure 3. R_{ct} of control cells, without additives, after formation and after 20 UHPC cycles. These are the control cells described in Figure 2.

without electrolyte additives after 20 UHPC cycles. Prior to dissection, the cells had been equilibrated at 50% state of charge, determined from the 20th cycle of the UHPC test. 50% state of charge was reached at 3.75 V for all cells. The positive-positive symmetric cells were made with the same electrolyte as the pouch cells from which the electrodes were harvested: $LiPF_6$, $LiBF_4$, or a 1:1 mixture of $LiPF_6$ and $LiBF_4$. The symmetric cells were cycled at 40°C, at a rate of C/10, between 0.5 V and −0.5 V, corresponding to full cell voltages of 3.25 V and 4.25 V. Figure 7 shows that the positive-positive symmetric cells with $LiPF_6$ fail within 10 cycles. The positive-positive symmetric cell with a 1:1 ratio of $LiPF_6$ and $LiBF_4$ failed after 30 cycles. Positive-positive symmetric cells with $LiBF_4$ completed 50 cycles without roll-over failure, sustaining less than 20% capacity fade. The cause of positive-positive symmetric cell failure may be impedance growth, as it has been shown that impedance growth occurs when positive electrodes are stored at high states of charge in the absence of the negative electrode.[30] In any case, Figure 6 shows that the parasitic reaction between the positive electrode and electrolyte which causes failure of positive electrodes with $LiPF_6$ does not occur, or is dramatically slowed, with electrolyte containing $LiBF_4$. This result is consistent with other studies, which have shown that organic carbonate solutions of $LiBF_4$ are more stable at high voltage than those of $LiPF_6$.[1,3,4,8,9]

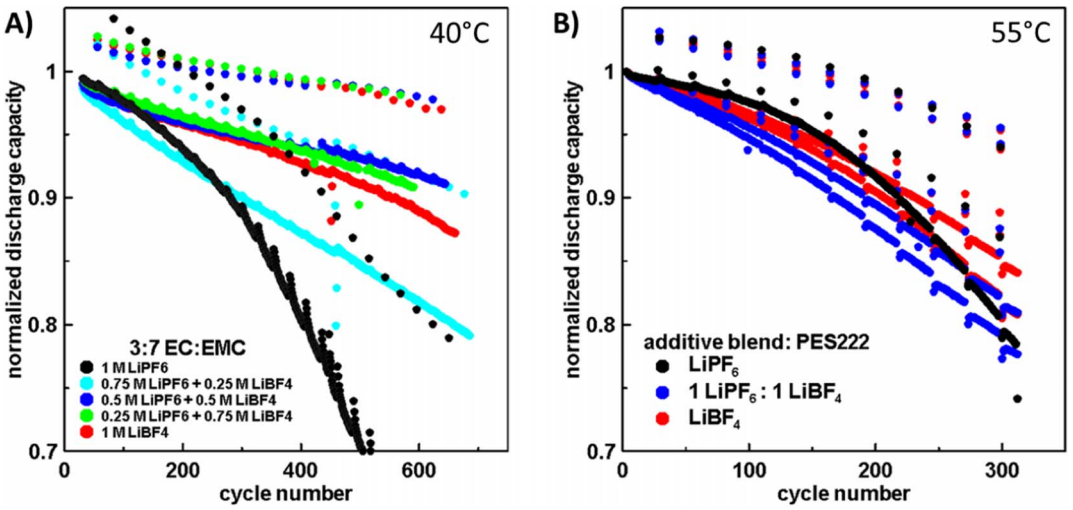

Figure 4. Normalized discharge capacity vs cycle number during long-term cycling for a) cells without electrolyte additives, cycled at 40°C and b) cells with PES222, cycled at 55°C, cycled at C/3 to 4.35 V.

This result also agrees with the UHPC data shown in Figure 2, which showed that cells with $LiBF_4$ had lower charge end point capacity slippage (electrolyte oxidation) than cells which contained $LiPF_6$ as the only salt. Reference 30 also showed that the presence of a negative electrode in a full cell "cleans" the electrolyte of harmful species, which is why the full cells in Figure 2 containing control electrolyte and $LiPF_6$ did not show roll-over failure in only a few cycles, unlike the symmetric cells.

Figures 7 and 8 show XPS data of electrodes from cells with control electrolyte without additives containing either $LiPF_6$ or $LiBF_4$ salts after 20 UHPC cycles. The electrodes were harvested from cells at 50% state of charge. Figure 7 shows data from the negative electrodes. The C1s spectra of the negative electrode SEI from the cell with $LiPF_6$ shows a large peak at 284.2 eV, corresponding to lithiated graphite, LiC_6. The C1s spectrum of the negative electrode from the cell with $LiBF_4$ has a much smaller peak in this position. This indicates that the negative electrode SEI in the cell with $LiBF_4$ electrolyte is much thicker than the SEI formed in the cell with $LiPF_6$, diminishing the observed intensity of the signal attributed to the underlying graphite. The thicker SEI formed by $LiBF_4$ electrolyte indicates that the initial SEI formed by $LiBF_4$ is not as effective at passivating the electrode, which causes continuous decomposition of electrolyte and thickening of the SEI over time. This could explain why symmetric cells made from negative electrodes cycled in $LiBF_4$ electrolyte have much larger R_{ct} than those cycled in $LiPF_6$, and why cells with $LiBF_4$ have greater first cycle irreversible capacity than cells with $LiPF_6$.[5] Figure 7 also shows that the negative electrode SEIs from cells with $LiBF_4$ and $LiPF_6$ differ greatly in chemical composition. The negative electrode SEI from the cell with $LiBF_4$ has more O-C = O (ester) species judging from the larger intensity near 533 eV in the O 1s spectra. The negative electrode SEI formed by $LiPF_6$-containing electrolyte has more inorganic oxides, carbonates or phosphates, judging from the larger intensity at 529 eV and 531 eV in the O 1s spectra. All these observations could be explained if Equation 1 occurred (adapted from Ref. 31).

$$R_2CO_3 + LiPF_6 \rightarrow CO_{2(g)} + POF_{3(g)} + 2\,RF + LiF\,(R = Li \text{ or organic}) \quad [1]$$

Equation 1 could account for the relative absence of carbonate or hemi-carbonate type groups and thinning of the negative electrode SEI in $LiPF_6$-based electrolyte. It is possible that this reaction occurs with $LiBF_4$-based electrolyte, but to a lesser extent, as $LiBF_4$ is more thermally stable.[13] The negative electrode SEI formed by $LiBF_4$ has ~9 relative atomic% of boron, while the negative electrode SEI formed by $LiPF_6$ has ~4 relative atomic% phosphorous. The F 1s spectra show that there are more fluoroborate species in the SEI formed in

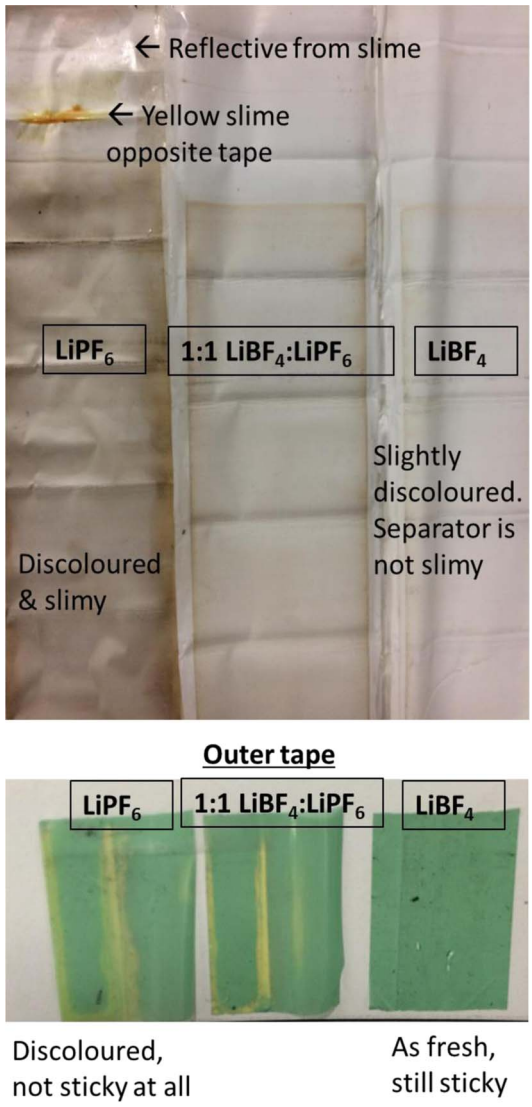

Figure 5. Separator and tape taken from pouch cells without additives, containing $LiPF_6$, 1:1 $LiPF_6$:$LiBF_4$ or $LiBF_4$, after 20 UHPC cycles at 40°C, to 4.35 V, at a rate of C/20. Separator and tape from the cell with $LiPF_6$ are the most discolored.

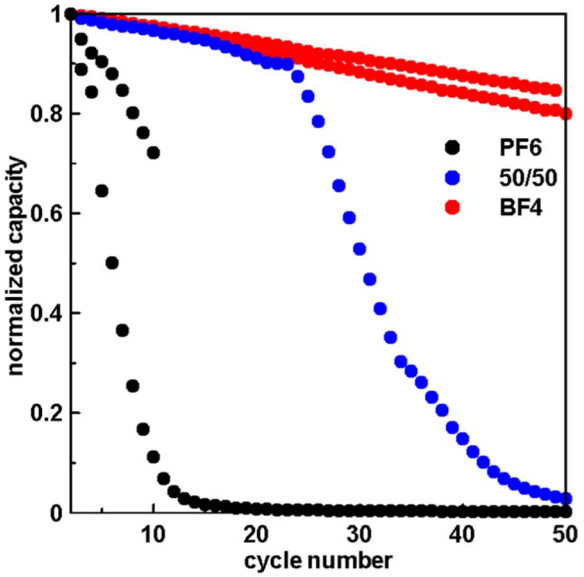

Figure 6. Normalized capacity of positive-positive symmetric cells, made with electrolyte without additives, containing $LiPF_6$, 1:1 $LiPF_6$:$LiBF_4$ or $LiBF_4$, cycled +/− 0.5 V.

$LiBF_4$ than fluorophosphates species in the SEI formed by $LiPF_6$. This may be a sign that the BF_4^- anion is not stable at the negative electrode. This can be rationalized if it is believed that species which coordinate strongly with Li^+ are reduced upon intercalation of Li^+, to form the negative electrode SEI.[32,33] Since $LiBF_4$ has a relatively small dissociation constant, BF_4^- is closely bound to Li^+ and may decompose as Li^+ is reduced.

Figure 8 shows XPS data of the positive electrode SEIs from cells with control electrolyte and $LiBF_4$ and $LiPF_6$. The chemical compositions of the positive electrode SEI are similar, except that the positive electrode SEI formed in $LiPF_6$ electrolyte has more of a C-O component, evidenced by the peak at 286 eV in the C1s spectra. The presence of this species apparently thickens the positive electrode SEI formed in $LiPF_6$ electrolyte. The relative thickness of the positive electrode SEIs can be gauged by the comparing the heights of the peak at 529 eV, attributed to the oxide in the NMC. The 3p peaks of Ni, Co and Mn are also half as intense in the spectrum of the positive electrode from the cell with $LiPF_6$, indicating that a thicker SEI covers this electrode. The chemical reaction which causes the thickening of the positive electrode in $LiPF_6$-based electrolyte could be related to the increased gas evolution at high voltage during the formation cycle (shown in Figure 1), the increased charge slippage during UHPC cycling (shown in Figure 2) and the poor performance of $LiPF_6$ electrolyte in positive-positive symmetric cells (shown in Figure 6).

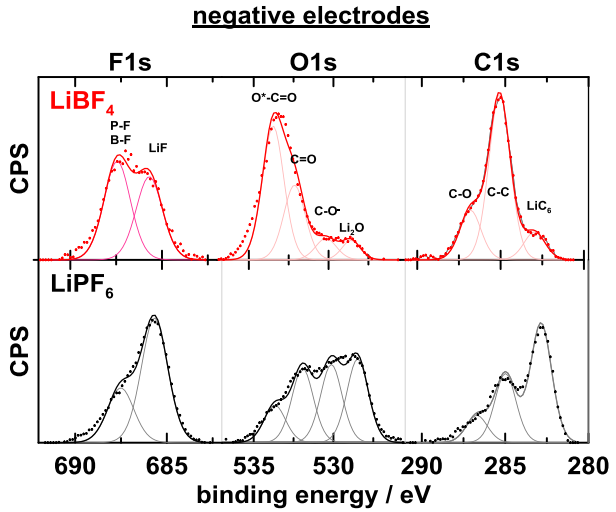

	Negative Electrode	
At %	$LiPF_6$	$LiBF_4$
F 1s	27.7 ± 0.6	26 ± 1
O 1s	27.3 ± 0.8	22.9 ± 0.8
C 1s	41.5 ± 0.9	42 ± 1
B1s/P2p	3.5 ± 0.9	9 ± 1

Figure 7. XPS spectra of negative electrodes after UHPC cycling in cells without additives, containing $LiPF_6$ or $LiBF_4$ electrolyte.

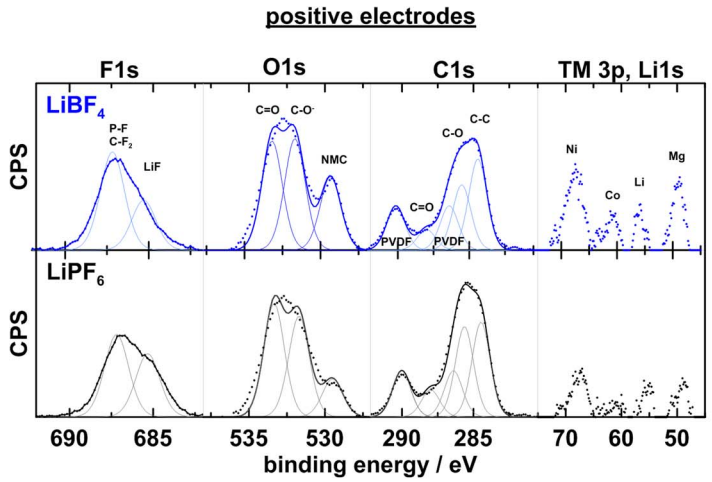

	Positive Electrode	
At %	$LiPF_6$	$LiBF_4$
F 1s	28.8 ± 0.7	29.6 ± 0.7
O 1s	15.9 ± 0.4	18.7 ± 0.5
C 1s	46.9 ± 0.9	41.9 ± 0.8
B1s/P2p	1.7 ± 0.4	0.8 ± 0.1
Li 1s	6 ± 1	7 ± 1
Ni 3p	0.4 ± 0.1	0.9 ± 0.1
Co 3p	0.2 ± 0.1	0.4 ± 0.1
Mn 3p	0.5 ± 0.1	1 ± 0.1

Figure 8. XPS spectra of positive electrodes after UHPC cycling in cells without additives, containing $LiPF_6$ or $LiBF_4$ electrolyte.

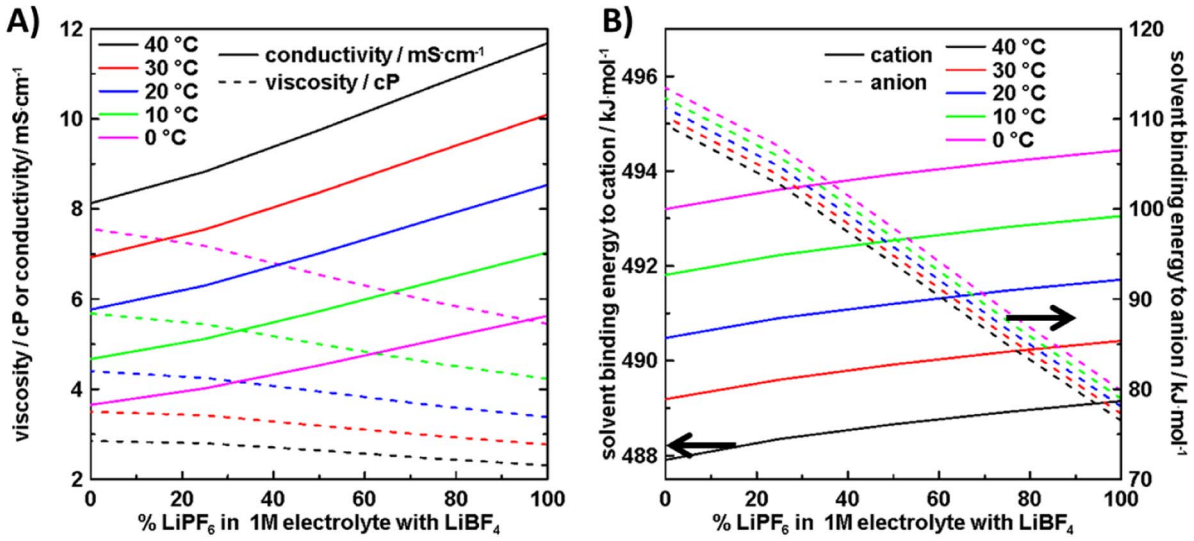

Figure 9. a) viscosity and conductivity, and b) anion and cation binding energy for control electrolyte (1 M salt in 3:7 EC:EMC), with various ratios of $LiPF_6$:$LiBF_4$. These results were calculated with Gering's Advanced Electrolyte Model (v. 2.172).

Figure 9 shows results of calculations using Gering's Advanced Electrolyte Model (AEM) (v. 2.172) on solutions of 3:7 EC:EMC containing 1 M solutions of various ratios of $LiPF_6$ and $LiBF_4$ at different temperatures.[18,19] Figure 9a shows conductivity and viscosity as a function of $LiPF_6$ content. Increasing amounts of $LiPF_6$ give increased conductivity and decreased viscosity, which is in agreement with previous studies.[34] From conductivity and viscosity, one would conclude that electrolytes based on $LiPF_6$ alone would perform better than $LiPF_6$-$LiBF_4$ blends. Figure 9b shows the average binding energy of the solvent molecules to Li^+ and the anions in the electrolyte with various ratios of $LiPF_6$ and $LiBF_4$. With increasing $LiPF_6$ concentration, the cation binding energy increases slightly. This could explain why the negative electrode SEI is formed by mostly organic species (which are subsequently consumed by $LiPF_6$, by Eq. 1), as it is thought that the negative electrode SEI is formed by the species which coordinate the most strongly to Li^+.[32,33] The opposite trend occurs for solvent binding energy to the anion: with increasing $LiBF_4$ concentration, the binding energy increases. It could be that strong bonding of the solvent to BF_4^- at the positive electrode prevents the oxidation of solvent molecules at the positive electrode. Figure 9b indicates there is a consequence to the competition between cation and anion for solvators: higher content of $LiBF_4$ results in higher relative solvent binding to the smaller anion, resulting in a modest decrease in cation solvation binding energy, and visa-versa. Also of note is the impact of temperature on solvent binding energies. They are greater at lower temperature due to increased stability of the solvated ion structures when thermal energy is decreased.

Conclusions

The effect of changing $LiPF_6$:$LiBF_4$ mole ratios in 1.0 M electrolyte, with 3:7 EC:EMC solvent, was studied in NMC442/graphite pouch cells cycled to 4.35 V. Use of $LiBF_4$ as the sole salt appeared to have good effects at the positive electrode. Cells with $LiBF_4$ as the sole salt produced less gas at high voltage during the formation cycle, had lower charge end point capacity slippage in UHPC cycling, and had a thinner positive electrode SEI compared to cells with $LiPF_6$ as the sole salt. Positive-positive symmetric cells with $LiBF_4$ salt in control electrolyte sustained 50 cycles with minimal capacity fade, whereas symmetric cells with $LiPF_6$ as the sole salt in control electrolyte failed within 20 cycles. Increasing amounts of $LiBF_4$ were observed to reduce discoloration of the separator and tape in cells without electrolyte additives after cycling. However, addition of $LiBF_4$ to the electrolyte appeared to have bad effects at the negative electrode. Increasing amounts of $LiBF_4$ caused larger irreversible capacity loss, increased R_{ct} after cycling in cells with control electrolyte, and a thicker negative electrode SEI.

Interestingly, the best performance in UHPC cycling experiments was obtained when the electrolyte contained an equal mole ratio of $LiPF_6$ and $LiBF_4$. These cells had the highest CE after 20 UHPC cycles. Cells with control electrolyte (no additives) and 1:1 $LiPF_6$:$LiBF_4$ had slightly worse CE after 20 cycles as cells with $LiPF_6$ and PES222–an effective electrolyte blend for high voltage cycling. In cells with control electrolyte and 2% VC, 1:1 $LiPF_6$:$LiBF_4$ resulted in the lowest charge-end point capacity slippage. This trend was observed again in long-term cycling experiments, where cells with control electrolyte and 1:1 $LiPF_6$:$LiBF_4$ cycled for 600 cycles with the least amount of capacity fade. We believe that the synergy between $LiPF_6$ and $LiBF_4$ is caused by the aforementioned benefits $LiBF_4$ imparts to the positive electrode, and the benefits $LiPF_6$ imparts to the negative electrode. Future work on this electrolyte blend should include more long-term cycling studies, to determine whether the synergy between $LiBF_4$ and $LiPF_6$ is present in many cell types and in many solvent blends. Investigations into the reactions of $LiPF_6$ and $LiBF_4$ at the negative and positive electrodes, and computational studies to investigate the synergism of the two salts, would be of use to further improve the understanding of the phenomena described in this paper.

References

1. X. Zuo, C. Fan, J. Liu, X. Xiao, J. Wu, and J. Nan, *J. Electrochem. Soc.*, **160**, A1199 (2013).
2. R. W. Schmitz, P. Murmann, R. Schmitz, R. Müller, L. Krämer, J. Kasnatscheew, P. Isken, P. Niehoff, S. Nowak, G.-V. Röschenthaler, N. Ignatiev, P. Sartori, S. Passerini, M. Kunze, A. Lex-Balducci, C. Schreiner, I. Cekic-Laskovic, and M. Winter, *Prog. Solid State Chem.*, **42**, 65 (2014).
3. Ş. Karaal, H. Köse, A. O. Aydin, and H. Akbulut, *Mater. Sci. Semicond. Process.*, **38**, 397 (2015).
4. T. Doi, Y. Shimizu, M. Hashinokuchi, and M. Inaba, *J. Electrochem. Soc.*, **163**, A2211 (2016).
5. L. D. Ellis, J. Xia, A. J. Louli, and J. R. Dahn, *J. Electrochem. Soc.*, **163**, A1686 (2016).
6. H. Zhou, K. Xiao, and J. Li, *J. Power Sources*, **302**, 274 (2016).
7. T. Doi, Y. Shimizu, M. Hashinokuchi, and M. Inaba, *J. Electrochem. Soc.*, **164**, A6412 (2017).
8. T. Ma, G.-L. Xu, Y. Li, L. Wang, X. He, J. Zheng, J. Liu, M. H. Engelhard, P. Zapol, L. A. Curtiss, J. Jorne, K. Amine, and Z. Chen, *J. Phys. Chem. Lett.*, **8**, 1072 (2017).
9. O. Borodin, W. Behl, and T. R. Jow, *J. Phys. Chem. C*, **117**, 8661 (2013).

10. C. L. Campion, W. Li, and B. L. Lucht, *J. Electrochem. Soc.*, **152**, A2327 (2005).
11. B. Ravdel, K. Abraham, R. Gitzendanner, J. DiCarlo, B. Lucht, and C. Campion, *Journal of Power Sources*, **119–121**, 805 (2003).
12. S. S. Zhang, K. Xu, and T. R. Jow, *J. Power Sources*, **159**, 702 (2006).
13. S. S. Zhang, K. Xu, and T. R. Jow, *J. Electrochem. Soc.*, **149**, A586 (2002).
14. S. Zhang, K. Xu, and T. Jow, *J. Solid State Electrochem.*, **7**, 147 (2003).
15. T. R. Jow, M. S. Ding, K. Xu, S. S. Zhang, J. L. Allen, K. Amine, and G. L. Henriksen, *J. Power Sources*, **119–121**, 343 (2003).
16. S. S. Zhang, K. Xu, and T. R. Jow, *J. Power Sources*, **156**, 629 (2006).
17. M. Mohamedi, D. Takahashi, T. Itoh, and I. Uchida, *Electrochimica Acta*, **47**, 3483 (2002).
18. K. L. Gering, *Electrochimica Acta*, **51**, 3125 (2006).
19. K. L. Gering, *Electrochimica Acta*, **225**, 175 (2017).
20. C. P. Aiken, J. Self, R. Petibon, X. Xia, J. M. Paulsen, and J. R. Dahn, *J. Electrochem. Soc.*, **162**, A760 (2015).
21. J. Self, C. P. Aiken, R. Petibon, and J. R. Dahn, *J. Electrochem. Soc.*, **162**, A796 (2015).
22. C. P. Aiken, J. Xia, D. Y. Wang, D. A. Stevens, S. Trussler, and J. R. Dahn, *J. Electrochem. Soc.*, **161**, A1548 (2014).
23. D. R. Lide, *CRC handbook of chemistry and physics*, CRC press, (2004).
24. R. Petibon, C. P. Aiken, N. N. Sinha, J. C. Burns, H. Ye, C. M. VanElzen, G. Jain, S. Trussler, and J. R. Dahn, *J. Electrochem. Soc.*, **160**, A117 (2013).
25. J.-M. Atebamba, J. Moskon, S. Pejovnik, and M. Gaberscek, *J. Electrochem. Soc.*, **157**, A1218 (2010).
26. N. Ogihara, S. Kawauchi, C. Okuda, Y. Itou, Y. Takeuchi, and Y. Ukyo, *J. Electrochem. Soc.*, **159**, A1034 (2012).
27. A. J. Smith, J. C. Burns, S. Trussler, and J. R. Dahn, *J. Electrochem. Soc.*, **157**, A196 (2010).
28. A. J. Smith, J. C. Burns, D. Xiong, and J. R. Dahn, *J. Electrochem. Soc.*, **158**, A1136 (2011).
29. L. Ma, D. Y. Wang, L. E. Downie, J. Xia, K. J. Nelson, N. N. Sinha, and J. R. Dahn, *J. Electrochem. Soc.*, **161**, A1261 (2014).
30. D. J. Xiong, R. Petibon, M. Nie, L. Ma, J. Xia, and J. R. Dahn, *J. Electrochem. Soc.*, **163**, A546 (2016).
31. S. Leroy, F. Blanchard, R. Dedryvere, H. Martinez, B. Carre, D. Lemordant, and D. Gonbeau, *Surf. Interface Anal.*, **37**, 773 (2005).
32. A. von Cresce and K. Xu, *Electrochem. Solid-State Lett.*, **14**, A154 (2011).
33. K. Xu, Y. Lam, S. S. Zhang, T. R. Jow, and T. B. Curtis, *J. Phys. Chem. C*, **111**, 7411 (2007).
34. K. Xu, *J. Electrochem. Soc.*, **154**, A162 (2007).